FIRST-PRINCIPLES STUDY ON THE ELECTRONIC STRUCTURE OF FeSe UNDER PRESSURE

BY

HABTAMU BEYENE

A THESIS SUBMITTED TO APPLIED PHYSICS PROGRAM

SCHOOL OF APPLIED NATURAL SCIENCE

PRESENTED IN PARTIAL FULFILLMENT OF THE REQUIREMENTS FOR THE DEGREE OF MASTER'S OF SCIENCE in PHYSICS

OFFICE OF GRADUATE STUDIES
ADAMA SCIENCE AND TECHNOLOGY UNIVERSITY

ADAMA, ETHIOPIA
AUGUST, 2017

FIRST-PRINCIPLES STUDY ON THE ELECTRONIC STRUCTURE OF FeSe UNDER PRESSURE

BY

Habtamu Beyene

Advisor : Mesfin Asfaw(PhD)

A THESIS SUBMITTED TO APPLIED PHYSICS PROGRAM

SCHOOL OF APPLIED NATURAL SCIENCE

PRESENTED IN PARTIAL FULFILLMENT OF THE REQUIREMENTS FOR THE DEGREE OF MASTER'S OF SCIENCE in PHYSICS

OFFICE OF GRADUATE STUDIES
ADAMA SCIENCE AND TECHNOLOGY UNIVERSITY

ADAMA, ETHIOPIA

AUGUST, 2017

FIRST-PRINCIPLES STUDY ON THE ELECTRONIC STRUCTURE OF IRON-SELENIUM UNDER PRESSURE

By

Habtamu Beyene

A THESIS SUBMITTED TO

APPLIED PHYSICS PROGRAM

SCHOOL OF APPLIED NATURAL SCIENCE

PRESENTED IN PARTIAL FULFILLMENT OF THE REQUIREMENTS

FOR THE DEGREE OF

MASTER OF SCIENCE in PHYSICS

OFFICE OF GRADUATE STUDIES

ADAMA SCIENCE AND TECHNOLOGY UNIVERSITY

ADAMA, ETHIOPIA

SEPTEMBER 2017

ADAMA SCIENCE AND TECHNOLOGY UNIVERSITY

DEAPRMENT OF PHYSICS

The undersigned hereby certify that they have read and recommend to the Faculty of Science for acceptance a thesis entitled "**FIRST-PRINCIPLES STUDY ON THE ELECTRONIC STRUCTURE OF IRON-SELENIUM UNDER PRESSURE** " by **Habtamu Beyene Master of Science**.

Dated: September 2017

Supervisor: _____
Dr Mesfin Asfaw

Readers: _____

_____

ADAMA SCIENCE AND TECHNOLOGY UNIVERSITY

Date: **September 2017**

Author: **Habtamu Beyene**

Title: **FIRST-PRINCIPLES STUDY ON THE ELECTRONIC STRUCTURE OF IRON-SELENIUM UNDER PRESSURE**

Department: **Deaprment of Physics**

Degree: **M.Sc.** Convocation: **July** Year: **2017**

_____

Signature of Author

Table of Contents

List of Tables

List of Figures

Acknowledgements

Firstly, it is a great pleasure to express my special appreciations and thank my supervisor Dr Mesfin Asfaw, the chairman of the department of Applied Physics program, ASTU. I would like to thank him for his Unlimited and constructive guidance, advice, suggestions, comments, encouragement and the support he gave from his vast knowledge and experience.

I would further thank ADAMA SCIENCE AND TECHNOLOGY UNIVERSITY (ASTU), Department of Applied Physics program and w/r Yetinayet, secretary of the department for her help through out my contact with department.and also I would like to thank Fikiru B., Getahun A.,Mekonnin A., Gosa R and others, for their support while I was a graduate student..

Finally, I would like to express thanks from bottom of my heart to all my family members, especially, Kiya and Sinbo for their love, and continues support. Above all I thank my Lord to his eternal love, kindness and support.

Habtamu B.W
Adama Science and Technology University
August, 2017

Abstract

This work focuses on the study of the band structure and superconductivity of FeSe under pressure(varying atomic position). We have performed density functional theory(DFT) calculations as implemented in QUANTUM ESPRESSO to calculate the electronic structure of the iron-based superconductor Iron-Selenium (FeSe). In our study, we have performed a comprehensive set of calculations involving how pressure influences on the electronic structure and the lattice dynamics properties of FeSe. All calculations were executed using the tetragonal lead-oxide or P4/nmm structure, with lattice parameters a and c, various volumes and c/a ratios, and found superconducting transition temperature of FeSe(T_c) increases sensitively under pressure from 8K to 16.75K at P$\cong$ 2Kbar, Furthermore, we investigated Fermi energy, total energies and pressure at ground state by using a pseudopotential method. We obtained comparable results with experimental in both calculations. Superconducting critical temperature T_c were calculated by using our DOS result in the McMillan formalism under pressure, our results show that the superconductivity critical temperature continues to rise. We also found that the equilibrium configuration of FeSe in the tetrahedral structure to have a volume of 75.49[Å^3] and 77.557[Å^3] with c/a ratio of 1.4889 and 1.552 in scf and optimization respectively. Thus obtained results are comparable to the experimental value(c:a = 1.47[a.u], V = 78.219[Å^3]. The density's at the Fermi energy are slightly enhanced under pressure. Zero pressure values of DOS at E_F are 2.69(state/cell/eV). At pressures corresponding to the maximum critical temperature, the density's equal to 3.54(state/cell/eV) (p$\cong$ 2Kbar).

keywords: superconductivity (SC), band structure, pressure effect, density of state(DOS) and critical temprature(T_c) .

Chapter 1

Introduction

From macroscopic point of view one can define Superconductivity as a phenomenon of zero electrical resistance in certain materials when cooled below a characteristic critical temperature T_c[1]. The mechanism of high-temperature superconductivity in the iron-based superconductors remains an outstanding issue in condensed matter physics. The electronic structure plays an essential role in dictating superconductivity.

Superconductivity is a quantum mechanical phenomenon. Hence, the electronic and magnetic properties of superconductors cannot be understood simply by classical physics of 'perfect conductivity'. The exclusion of the interior magnetic field can be explained by the Meissner effect, while the absence of the electrical resistance in a superconductor and the microscopic properties can be explained through the electron pairing via the electron-phonon interaction in the crystal lattice as explained by John Bardeen, Leon Cooper, and Robert Schrieffer, (BCS theory).

It was found that certain materials undergo a phase transition to a state with zero electrical resistance, R = 0, at a certain critical temperature, T_c. The electrical resistance is defined from the Ohm's law, resistivity, R=V/I, where V is the voltage and I is the current. The conductivity unit length in a wire, is the inverse of the resistivity. The current density$J = \sigma$E , where E is the electric field. In order to obtain zero resistance in the sample, the voltage across the sample must be zero. Then, this sample exhibits the character of a perfect conductor with a finite current flow without any energy loss. It was also found

that at relatively low temperature, $T < T_c$, the magnetic field inside the sample is zero. Any applied magnetic field on the sample was also found to be deflected from the samples. The phenomenon of the perfect conduction the exclusion of magnetic field in a material is called 'superconductivity' and the material that carries this phenomenon is known as a superconductor. Hence, superconductor can be distinguished from a perfect conductor by two very simple characteristics, which is the zero electrical resistance in the sample and the exclusion of the interior magnetic field.

The discovery of a new class of high-temperature superconductors iron based layered compounds aroused a significant interest at the beginning of 2008 gave hope for a progress in the synthesis of novel high-temperature superconductors (HTSC) up to room-temperature superconductors [2]. The nature of high-temperature superconductivity is not completely understood yet. The principal task of solid-state physics is the creation of superconductors which would ensure superconductivity at room temperature. Therefore, the large-scale search for such high-temperature superconductors is proceeding and intensified. The crucial role in the explanation of physical properties of superconductors is played by calculations of the electronic structure from the first principles. It is worth noting that one of the basic properties of high-temperature superconductors is the presence of a lot of bands [3].

The electronic structure of the iron-based compounds usually consists of hole-like bands near the Brillouin zone center and electron-like bands near the Brillouin zone corners, leading to proposals that the electron scattering between the hole pockets around the Brillouin zone center and the electron pockets around the Brillouin zone corners is a viable mechanism for electron pairing in the iron-based superconductors [4].

Different materials superconductivity at different critical temperatures exhibit different phase transitions, while keeping the general properties. Hence, superconductors can be further classified into two different types, which can be easily distinguished by their unique electronic and magnetic properties,

namely the Type I superconductor and the Type II superconductor. Type I superconductors generally superconductivity at lower temperatures and lower critical field while the type II superconductors superconductivity at a higher temperature range with higher critical field with two critical fields. Most of the pure metals in the periodic table such as mercury, tin and lead which are superconductors exhibit type-I superconductivity, whereas most alloys like lead-bismuth alloys, barium-copper-oxide ceramics and highly-doped semiconductors exhibit type-II superconductivity. Noble metals such as gold and silver do not exhibit superconductivity.

The highest T_c observed so far in the Fe-based systems is 55K[5]. Pressure has been found to be a powerful tool for superconducting properties of these compounds, since the application of external pressure can induce or enhance superconductivity[5]. Aiming at clarifying the role of the lattice with respect to the pressure-induced changes of the electronic properties, we have probed the high-pressure structural behavior of undoped Fe-based compound, namely FeSe, investigated at room temperature.

Later on, FeSe superconductor was found to have higher transition temperature when the Se vacancy is substituted with tellurium atoms. It was also found that FeSe becomes superconducting upon oxidation[6]. With application of pressure, the superconducting temperature was raised to $\sim$37K [6]. The conduction in iron-based superconductor is not explained by the periodic symmetry of the lattice structure but by doping and non-stoichiometry of the compound and also FeSe has been less widely studied than the 122 systems because of difficulties in single - crstal growth.

Here, we are interested to study effects of pressure on the atomic position of FeSe considering the peculiar nature of FeSe compounds with the physical properties due to the variation of the lattice and the inter atomic structural parameters that would have the appearance and suppression of superconductivity[7], in which one expect the appearance of many interesting and new physical phenomena when studying these materials under high pressure.

✠ General Objective:

The main aim of this study is to examine the pressure effect on electronic structure of FeSe in the normal state with in the density functional theory (DFT) calculations. It is meaningful to investigate how pressure influences the electronic structure and the lattice dynamics properties of FeSe from the ab-initio point of view.

✠ Specific Objectives:

The specifics objective are to be:

- Calculate band structure of FeSe compound with vary lattice parameters.
- State the relation between lattices parameter, Fermi energy, total energies, volume and pressure.
- Determine critical temperature of FeSe compound under pressure.
- Calculate electronic density of states for FeSe.

Chapter 2

Review of related literature

2.1 General Overview of Superconductivity.

2.1.1 Development in the story of superconductivity

In 1911, a Dutch physicist, Heike Kammerlingh Onnes did a study on the electronic property of metals at very low temperatures[7]. Upon studying the property of solid mercury, it was found that the resistance of the solid mercury in the liquid Helium drops gradually with the decrease of temperature. Upon reaching 4.2K, the electrical resistance of the solid Mercury drops abruptly to zero as shown in Fig.2.1. Hence, a perfect conductor that conducts current with zero resistance is found. Onnes named this phenomenon as 'superconductivity' and with this discovery which requires liquid helium; he was awarded with Nobel Prize for liquefying helium gas in 1913. Onnes' discovery ignited much interest among scientists to do more experimental work to study this phenomenon further as well as to understand theoretically the explanation of the physics behind the extraordinary discovery. Many more materials were found to be superconducting such as : lead with superconducting transition temperature at 7.19K in 1913 and niobium nitride with superconducting transition at 16K in 1941.

The understanding of superconductivity was taken to another notch by Walther Meissner and Ochsenfeld in 1933. By setting the current to run in a circular motion in a superconducting material, an internal magnetic field is formed. When the sample is cooled to the critical temperature T_c, the magnetic field

in the sample disappears and expels any external magnetic field as shown in Fig. 2.2. The exclusion of interior magnetic field is known as the Meissner effect[5].

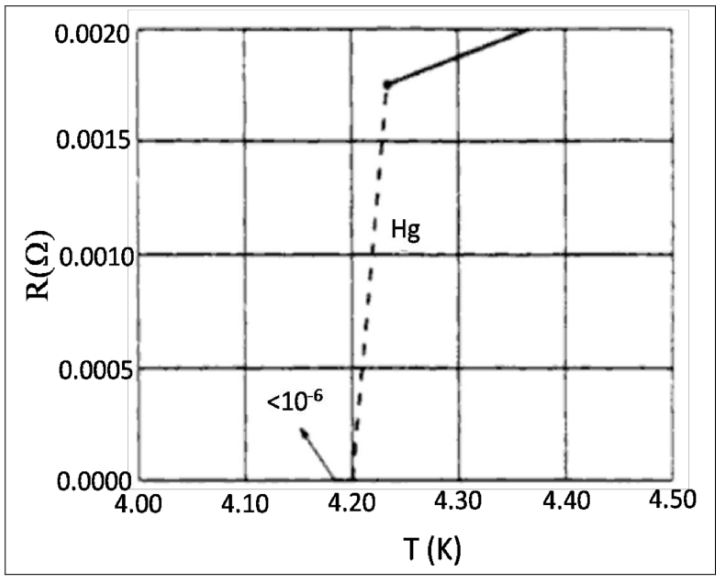

Figure 2.1: *The resistance, R versus temperature, T curve of Kammerlingh Onnes, Commun. Phys. Lab. Univ. Leiden, Nos. 122,124 (1911) indicating the superconducting transition phase in mercury.*

In the early 1950's B. Matthias discovered a correlation between T_c and the number of valence electrons per atom (R) of a large number of superconducting elements and compounds[8, 9]. While there was no superconducting compound with $R \leq 2$ at the time Matthias showed the existence of a maximum of T_c (R) close to R = 4.75[8] and a second maximum at $R \approx 6.4$[9]. Most of the intermetallic superconductors with a high T_c exhibit lattice instabilities. The application of external pressure to these high T_c superconductors can drive the compounds towards or away from lattice instabilities by varying the principal parameters determining the superconducting properties (the electronic density of states at the Fermi energy, $N(E_F)$, the characteristic phonon frequency, and the coupling constant of electrons and phonon's), and it can be used to tune the T_c and the superconducting properties. Almost all of the superconducting metallic elements show a decrease of T_c with pressure. This negative pressure coefficient was attributed to the volume dependence of $N(E_F)$

and of the effective interaction between the electrons mediated by the electron-phonon coupling [10]. However, a few elemental superconductors such as Tl and Re show a more complex pressure dependence of T_c that was explained by pressure-induced changes of the Fermi surface topology[11,12].

New techniques for creating higher pressures have been developed over the last couple of decades pushing the limits of static pressure generation to a few hundred GPa. At high enough pressure almost every ambient pressure structure becomes unstable and transforms into a structure of higher density and, frequently, of higher symmetry. Some elements or compounds undergo a sequence of structural transitions into several different phases under applied pressure. Many of these new structures are metallic and superconductivity was observed in a large number of high-pressure phases even when the compound was not superconducting at ambient pressure. Among the elements of the periodic table, superconductivity induced by pressure has raised the total number of superconducting elements from 29 (at ambient pressure) to 52 including non-metallic elements like sulfur or oxygen and alkali metals with only one valence electron such as Li.

The latter alkali metal is of particular interest since it is one of the elements of the first column of the periodic system that should not be superconducting according to the Matthias rules. In 1969 Allen and Cohen[13], based on their pseudopotential calculations, proposed Li to be superconducting but no evidence of superconductivity has been found at temperatures as low as 4mK[14]. However, it was predicted that superconductivity should occur in Li under high pressure with transition temperatures of up to 80K[15]. Early high-pressure experiments[15] revealed a drop of resistivity in Li at 7K between 22 and 32GPa but the data were not conclusive enough to be interpreted in terms of superconductivity. Only recent measurements of electrical transport and magnetic properties have unambiguously shown that superconductivity exists in Li at pressures above 20GPa and at temperatures up to 20K[17, 18,19]. The large interest in the superconductivity in dense lithium is also motivated by the fact that it is the "simplest" metal with only one valence electron, no d-electrons in sight, and it is the superconducting element

closest to hydrogen. There appears to be new hope in the continuous search for superconductivity in metallic hydrogen that has been predicted to become superconducting at high pressure with an extraordinary high T_c[20].

Experimental results alone are not enough to explain the unusual phenomenon of superconductivity. Many scientists join in the race to explain their theories. In 1950 Landau and Ginzburg gave a macroscopic explanation for the properties of superconductors by using the thermodynamic arguments, such as the concept of free energy[21]. From there, Abrikosov predicted the two divisions of the superconductors, which is today's type I and Type II superconductors. He also explains the penetration of magnetic flux in the type II superconductors. Also in the same year, Maxwell and Reynolds et al. found that the critical temperature of a superconductor is dependent on the isotopic mass, M, of the constituent element, T_c 1/ M.

Later in 1957, John Bardeen, Leon Cooper and Robert Schrieffer introduced the BCS theory that unveils the explanation for the mysterious conductivity in the superconductor by explaining the microscopic properties of superconductors[21]. By modelling the superconducting current as superfluid of Cooper pairs, the zero resistivity conduction is explained by a pair of electrons interacting through the exchange of phonons. The authors of BCS theory were later awarded the Nobel Prize in 1972.

The new area of superconductivity began in 1986 with the discovery of superconductivity in lanthanum-based cuprate perovskite material at 35K by Bednorz and Mueller[22]. The critical temperature was a lot higher than the previous record of 18K in Nb_3Sn and 23K for NbGe. Later in 1987, a perovskite ceramic material was found to superconduct at 92K.

In February 2008 the study of superconductivity shifted its focus from ceramic material to iron-based material. The new material was discovered by Hideo Hosono et al. of the Tokyo Institute of Technology when they found that lanthanum oxygen fluorine iron arsenide ($LaO_{1-x}F_xFeAs$) superconducts

at 26K[3]. Subsequent research was done by other scientists after the discovery of Hosono. Substitution of different rare earth materials into $LaO_{1-x}F_xFeAs$ brings the superconducting temperature to 52K. Many Fe-bearing compounds were found to be superconductors either upon varying the composition, such as the ternary iron-pnictide family AFe_2As_2 (A=Ba, Sr, Ca, Eu), or without doping, e.g. the FeSe and the LiFeAs compounds[5]. The highest T_c observed so far in the Fe-based systems is 55K[5].

In iron - based superconductors several studies on the effect of impurities have been carried out and it has soon emerged that the behavior may very a lot depending on the family considered. The most dramatic and yet not fully understood effect is introduced by Mn for Fe substitution in the optimally electron doped $LaFeAsO_{0.89}F{-}0.11$[23,24].

2.1.2 Meissner Effect

The Meissner effect was discovered in 1933 by Water Meissner and Robert Ochsnfield[25]. It is one of the properties of superconducting materials. When a superconductor below critical temperature (T_c) is placed under a weak external magnetic field B, it repels the magnetic flux (field) B completely from its interior. It does setting up electric currents near to surface. The magnetic field of these surface currents that cancels out the applied magnetic field with bulk of superconductor. However, near to the surface distance called the London penetration depth. The magnetic field is not completely canceled and this region also contains the electric currents, whose field cancels the applied magnetic field with in the bulk superconductivity. This exclusion of magnetic flux from superconductor(B = 0) is known as Meissner effect[26], as shown in fig.2.2.

$$(CGS)B = B_a + 4\pi M = 0 \tag{2.1}$$

$$\frac{M}{B_a} = \frac{-1}{4\pi}$$

$$B = B_a + \mu_0 M = 0 \tag{2.2}$$

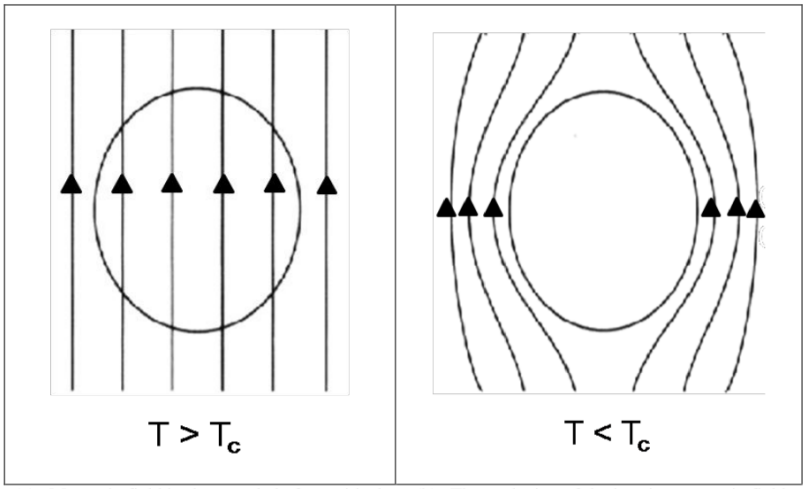

(a) Magnetic field in the sample before critical temperature

(b) The exclusion of the interior magnetic field at critical temperature

Figure 2.2: *The Meissner effect of (a) normal and (b)superconducting states ($T > Tc$ and $T < Tc$).*

The result B = 0 can not be derived from the characterize of superconductor as medium of zero resistivity. From Ohm's law $E = \rho_j$. We see that if the resistivity ρ goes to zero while current density(J) is held finite, E must be zero. By the Maxwell equation relation $\frac{dB}{dt} = \nabla \chi E = 0$, so that zero resistivity implies $\frac{dB}{dt} = 0$. This argument is not entirely transparent. But the result predicts that the flux through the metal can not change on cooling through the transition. The Meissner effect suggests that perfect diamagnetic is an essential property of the superconducting state[27].

2.1.3 BCS Theory of Superconductivity

The first successful microscopic explanation for the conduction in superconductivity was formulated by Bardeen, Cooper and Schrieffer in 1957. It is known as the BCS theory and it could quantitatively predict the properties of a superconductor. This theory is based on the formation of pairs of electrons of momenta k and -k with one electron spin up and the other spin down, proposed by Leon Cooper, which shows that there is instability of the Fermi surface at the ground state upon the formation of pairs of 'bound' state electrons. This bound pairs of electrons are attracted to each other via the electron-phonon interaction and it is also known as the Cooper pairs.

The zero resistance in superconductivity can be explained by the movement of these Cooper pairs through the lattice unaffected by the thermal vibrations. This is because at low temperatures, the attractive phonon interactions between the electrons are stronger than the interaction between the electron's and ions. Hence, the electron-phonon interactions overcome the Coulomb interaction. The formation of Cooper pairs can be explained by first explaining the distortion of the crystal lattice by a single electron in the lattices as shown in Fig.2.3. This distortion of the crystal lattice will form a charge distortion (phonon) of positive charges around the electron. This charge distortion will eventually attract another electron at a certain distance in the lattice forming bound pairs of electrons.

The formation of bound pairs can also be described as the interaction of

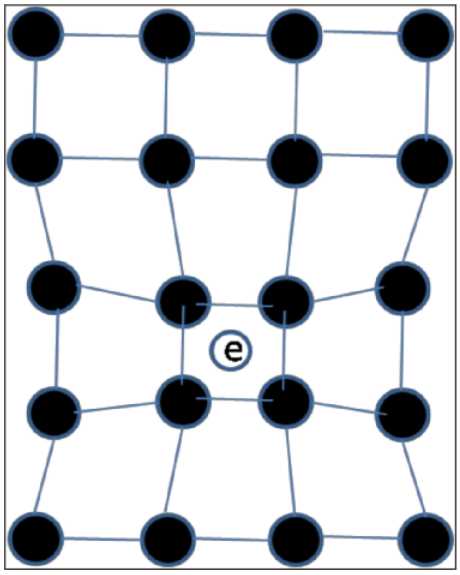

Figure 2.3: *Lattice distortion created by the single electron in the lattice.*

electrons due to the emission or absorption of lattice phonons. The emission and absorption process can be represented by the famous Feynman diagram as shown in Fig. 2.4.

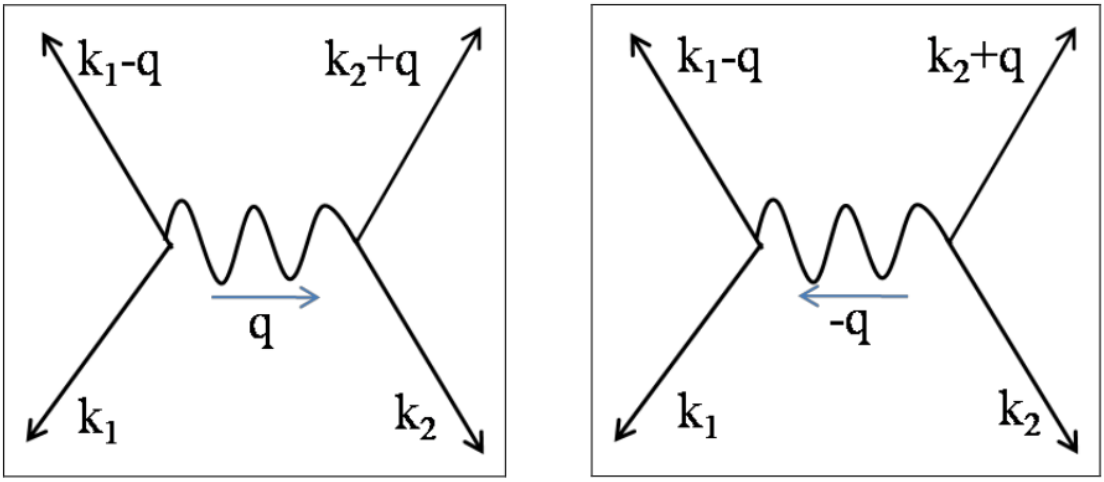

(a) Emission of phonon from the first electron (left to right).

(b) Absorption of phonon of the first electron from the second electron

Figure 2.4: *The Feynman diagrams in (a) and (b) are the mirror process of phonon emission and absorption between two electrons. k 1 , k 2 and q are the wave vectors.*

2.1.4 Classification of Superconductors

Superconductors can be classified into two types, namely the Type I superconductor and the Type II superconductor. Both superconductors share many common properties but show different magnetic behaviour. Type I superconductor exhibits zero resistivity and exclusion of magnetic field from the interior of the superconductor (Meissner effect) at relatively low temperature, namely below the critical temperature, T_c. This superconductor only has one critical field, H_c, where superconductivity is destroyed when the applied magnetic field is beyond that critical field value. The critical magnetic field varies with temperature.

For any field below the critical field, the magnetization is negative, giving a diamagnetic material. The microscopic properties of Type I superconductors are accurately described by the BCS theory and it is also known as the conventional superconductor.

Type II superconductors are somehow much more complicated than the Type I superconductors. Besides sharing the similarity of zero resistivity below the transition temperature, Type II superconductors have two critical fields, one

coming from the London penetration depth and the other from the coherence length. Due to scattering from the magnetic atoms, the transition temperature of the type-II superconductors is lower than those of type-I superconductors.

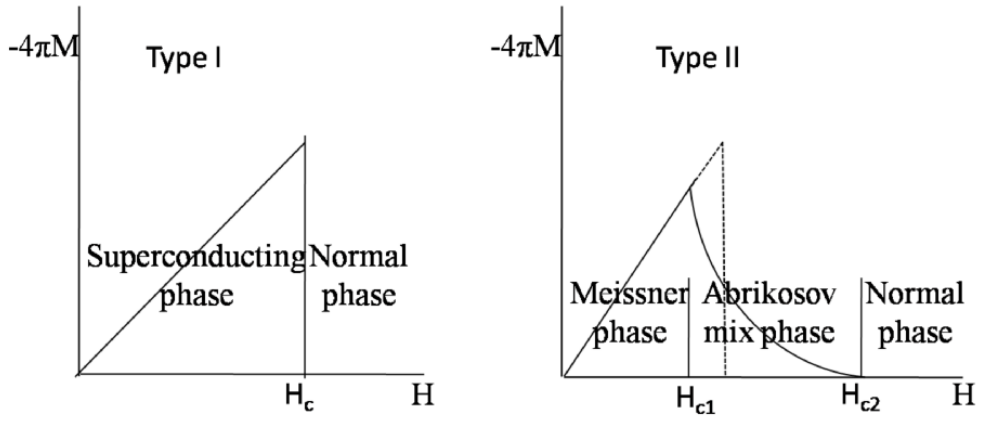

Figure 2.5: *The graphs show the magnetization curve of Type I and Type II superconductors with negative magnetization.*

In the Abrikosov mixed phase, the high temperature superconductor allows certain amount of magnetic field to penetrate the sample. Hence, this explains the higher upper critical field in the type-II superconductors. The BCS theory is not sufficient to explain the conduction in the high-temperature superconductor and hence, Type II superconductors are also known as the unconventional superconductors.

2.1.5 The Pressure Dependence of T_c in BCS and Strong-Coupling Theory of Superconductivity

Pressure is a very important thermodynamic parameter in solid state physics and is considered as an attractive variable, because the ground state of a system can be tuned without modifying the chemical composition. The basic microscopic effect of pressure on solids is to decrease the inter atomic distances, as well as change the bond angles. The pressure-induced variation in both of these structural parameters will usually increase the overlap between the electronic orbitals of adjacent atoms.

The pressure dependence of T_c can be derived from microscopic theories of phonon-mediated superconductivity such as the weak-coupling BCS model[28] or the Eliashberg theory of strong-coupling superconductivity[29]. For a specific superconductor the knowledge about the pressure dependence of its microscopic parameters such as the average phonon frequency, ω_D, the electronic density of states, N(E_F), etc. is then needed to estimate T_c as function of imposed pressure. According to the weak-coupling BCS theory T_c is expressed by[28]

$$K_B T_C = 1.13\hbar\omega_D exp(\frac{-1}{\lambda}) \tag{2.3}$$

No matter how weak the electron-phonon coupling, BCS predicts a transition to a superconducting state for an attractive interaction described by the attractive potential V_e where k_B and $\hbar$ are Boltzman's and Planck's constant, respectively, $\lambda = N(E_F)V_e$, and V_e is the effective interaction between the electrons mediated by the electron-phonon coupling. Since ω_D commonly increases with pressure (phonon hardening) the frequently observed decrease of T_c with pressure must be due to a decrease of λ. The average value of the electronic density of states is expected to decrease under pressure because of the pressure-induced band broadening effect. However, the pressure dependence of N(E) can be very different at the Fermi energy E_F, depending on the details and the topology of the Fermi surface in a particular compound. The pressure dependence of V_e is even more difficult to estimate and it needs a microscopic treatment of the coupled system of electrons and phonons. It should be noted that the BCS - equation (2.3) applies only in the weak-coupling case when the electron-phonon coupling constant λ is small.

Most superconducting elemental metals (except Al) exhibit an intermediate to strong electron-phonon coupling with λ of the order of 1 or larger[30] and their superconductivity is not well described by the weak-coupling BCS equation

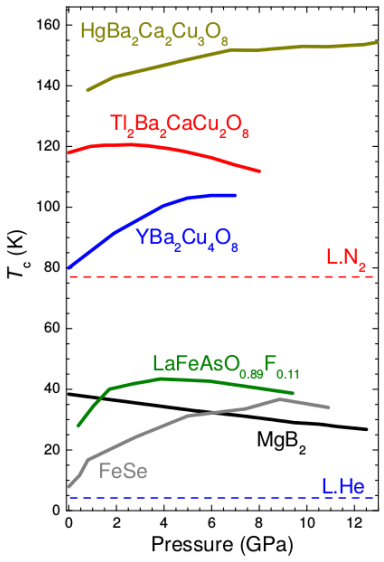

Figure 2.6: *Pressure dependence of the superconducting transition temperature T_c for selected superconductors[33].*

(2.3). Extending the original BCS theory[28], Eliashberg developed the theory of strong-coupling superconductivity[29] that provides, together with the pseudopotential treatment of the screened Coulomb interaction[31], the fundamental equations describing the physics of superconductors with phonon mediated pairing of any coupling strength. By solving the finite-temperature Eliashberg equations McMillan[32]:

$$K_B T_C = \frac{\Theta_D}{1.45} exp\{-\frac{1.04(1+\lambda)}{\lambda - \mu^*(1+0.62\lambda)}\} \tag{2.4}$$

$\mu*$ is the Coulomb pseudopotential calculated in [34]:

$$\mu* = 0.13\frac{N(E_F)}{1+N(E_F)} \tag{2.5}$$

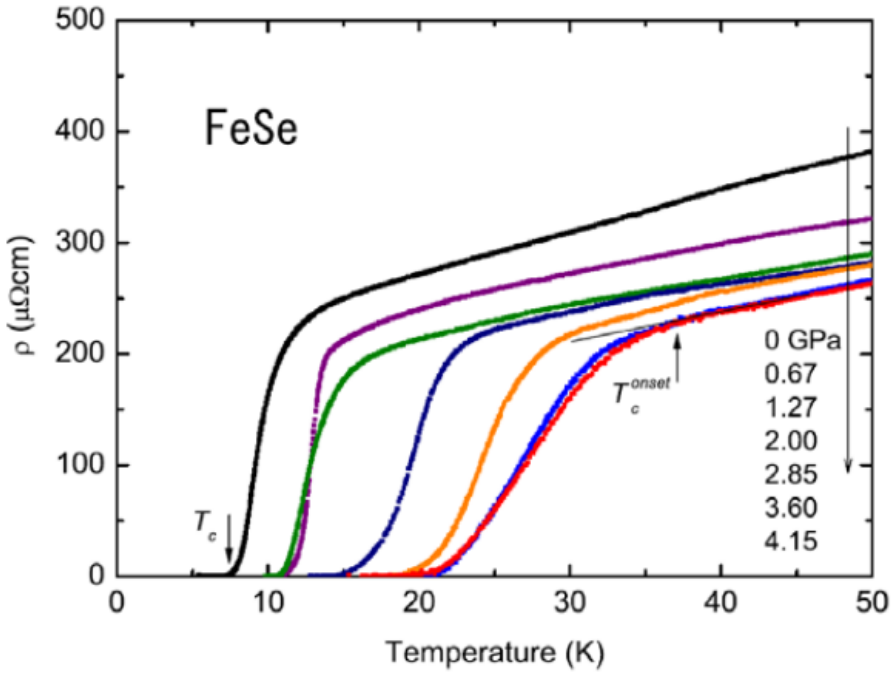

Figure 2.7: *Temperature dependence of resistivity measured using an indenter cell for FeSe under high pressure up to 4.15 GPa.[35]*

2.1.6 Iron based superconductors

Iron-based superconductors are iron-containing chemical compounds. The study on the iron based superconductors has got a great attention following the report on $LaFeAsO_{1-x}F_x$[36]. The highest superconducting critical temperature T_C reaches 56k[37] by replacing La with other rare earth elements Ce, Pr, Nd, Sm, and Gd. This class of material provides a large number of superconducting compounds that are grouped in general stoichiometry of LnFeAsO ("1111") family (eg. Ln = La), MFe_2As_2 ("122") family(eg. M = Ba), MFeAs ("111") Family (eg. M = Li), and FeM ("11") family (eg. M = Se)[38-41]. Both families of iron pnictides have a quasi-two-dimensional (2D) tetragonal crystal structure. Fig (2.8) shows crystal structure of the main families of pnictides. The parent compound LaFeAsO contains FeAs layers sandwiched by LaO layers. Each FeAs layer consists of a square-lattice Fe plane with As atoms above and below the plane alternatively.

The common feature of these main families of Iron based superconductors(the 1111, 122, 111, and 11 families of materials) is the presence of an identical

FeAs (or FeSe) plane. It was reported that these families of iron based superconductors attain different value of superconducting temperature T_C (table 2.1).

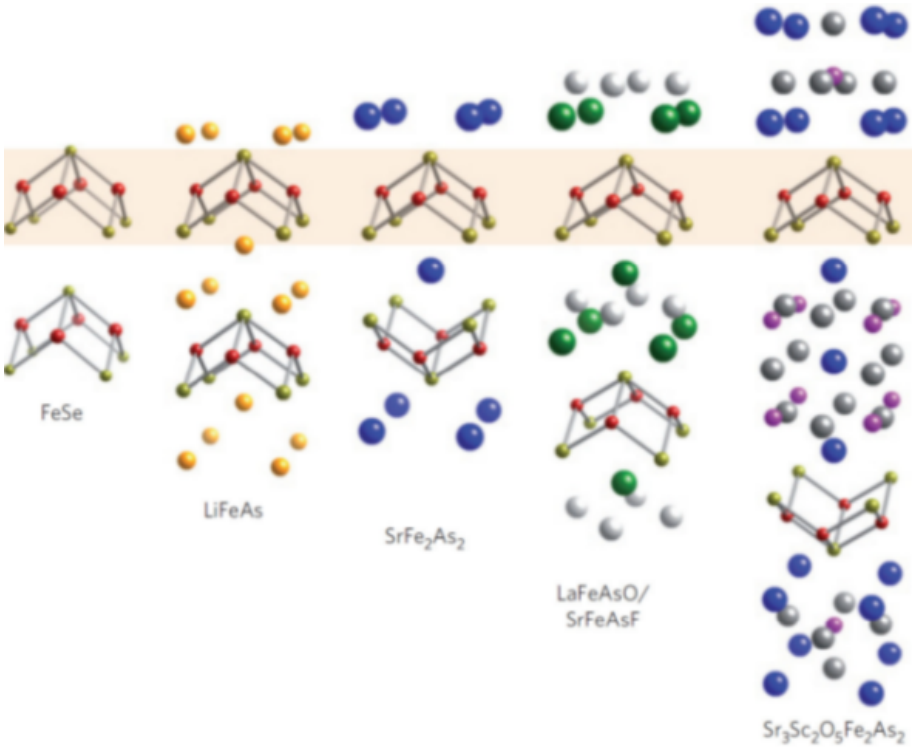

Figure 2.8: *Crystal structures of some of iron-based superconductors(taken from Ref.[42]*

Table 2.1: *The maximum T_C for the main families of iron based superconductors yet found(taken from ref (43)).*

Compounds	Familiy type	Maximum T_C
RFeAsO	1111	57K
$AFe-2As_2$	122	38K
LiFeAs	111	25K
FeSe	11	15K

In many publications, much effort has been made theoretically and experimentally to identify the main cause of novel properties of materials. A deeper understanding on the doping effect of the electronic structure of this systems can provide insight into the interplay between magnetism and Superconductivity.

2.1.7 Superconductivity of FeSe compound.

In February 2008, the study of superconductivity shifted its focus from ceramic material to iron-based material. The new material was discovered by Hideo Hosono et al. of the Tokyo Institute of Technology when they found that lanthanum oxygen fluorine iron arsenide ($LaO_1 - xF_xFeAs$) superconducts at 26K[44]. Subsequent research was done by other scientists after the discovery of Hosono. Substitution of different rare earth materials into $LaO_1 - x$ F_xFeAs brings the superconducting temperature to 52K. Different type of iron-based materials such as FeS, FeSe and FeTe were also studied[45].

Since the discovery of superconductivity in $LaFeAsO_1 - xF_x$, FeAs compounds which have a structure similar to LaFeAsO have been confirmed to show superconductivity at the comparably high transition temperature T_c[46-51]. They commonly contain anti-PbO-type FeAs layers as the superconducting layers in its crystal structure.In July 2008, Hsu et al. reported the superconductivity at 8K in anti-PbO-type FeSe[2]. α-FeSe is composed of only the FeSe layers with the anti-PbO-type structure (space group: P4/nmm).

The crystal structure of FeSe is the simplest among Fe-based superconductors. Furthermore, the theoretical study indicated the similarity in the electronic states between Fe chalcogenides (FeS, FeSe and FeTe) and the FeAs-based superconductors[52]. The contributions of Fe-3d electrons near the Fermi level E_F and the morphology of the Fermi surface exhibited similarities to the FeAs-based superconductors. Because of these natures common to the FeAs-based superconductors, the FeSe superconductor has attracted a lot of researchers as the key material to elucidate the mechanism of Fe-based superconductivity.

FeSe superconductor has attracted extensive attention for similar to those

FeAs layer. The FeSe superconducting transition temperature exhibits a compositional dependence, decreasing for both under doped and over doped material[15] as observed in the cuprate. Superconductivity show only, when prepared with deficiency of selenium (Se) and substituting doping of electron from Tellurium (Te) element. For polycrystalline of FeSe sample compound can increase T_c value with applying pressure. Therefore the value of T_c strongly depends on the applied pressure, and the temperature at which the resistivity becomes zero

2.1.8 Band structure and DOS of FeSe superconductors

In 2008, the new class of iron-based superconductors was discovered. One of the representatives of this class is FeSe compound distinguished by the simplest crystal structure among iron-based superconductors and by the extremely large effect of a pressure on the superconducting transition temperature[53]. The basic structural feature connecting the Fe-based superconductors is the presence of square planar sheets of Fe coordinated tetrahedrally by pnictogens or chalcogens and nominal Fe valence near Fe^{2+}. The structure of FeSe, that is the simplest of the compounds, consists of square planes of Fe with Se atoms arranged above and below the planes in such as way as to tetrahedrally coordinate the iron. The structure places the Fe atoms closer together than in a perovskite, so that direct Fe-Fe interactions are important.

Electronic band structure calculation has been popular after the discovery of DFT in 1960. It is one of the important parameter to study various properties of materials, such as electrical and structural. First principal calculation leads to obtain electronic band structure and Fermi surfaces. Fig.(2.9) shows the band structure of FeSe, reproduced by the concept of non spin unpolarized calculation[54]. The result of the calculation shows that Fe 3d orbital bands are present near the Fermi energy. The figure also shows 5 bands are crossing the Fermi level, that depicts the multi band nature of the iron based compounds.

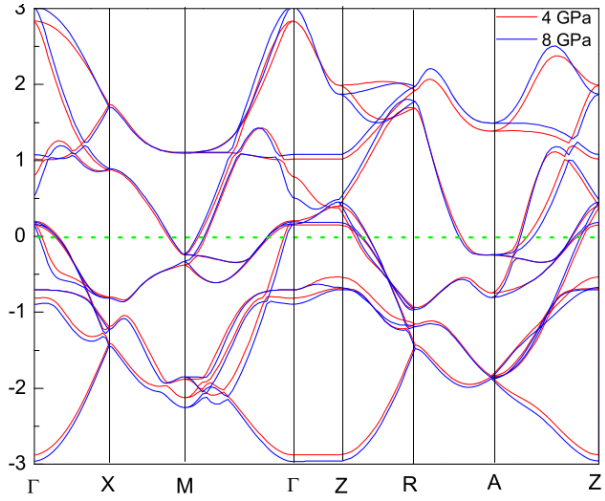

Figure 2.9: *The electronic band structures of FeSe along high-symmetry lines at P = 4GPa, 8GPa. The Fermi energy is set to be zero[45].*

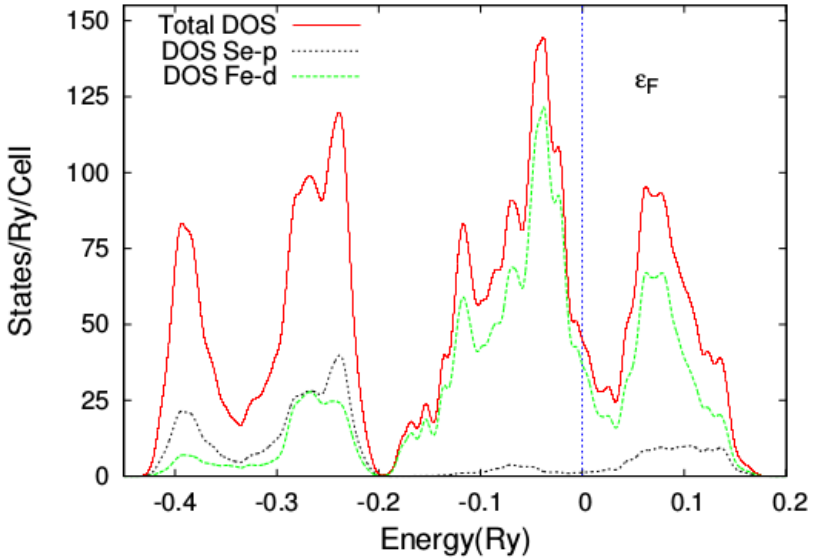

Figure 2.10: *Total, Se-p, and Fe-d density of states of FeSe at ambient pressure. Notice that the Fe-d component is the largest contributor to the total DOS around the Fermi level. Dashed vertical (blue) line represents the Fermi level[55].*

Density of State(DOS) in superconductivity is an important parameter to understand several properties. If the number of DOS near the Fermi level is changing, for instance by doping, then the properties of the material may change dramatically. Applying Density Functional theory as implemented in Quantum Espresso(QE) code one can calculate the DOS of a compounds, as shown in Fig 2.10 for FeSe.

2.1.9 Applications

After the discoveries of new superconducting materials and the gradual improvement in theoretical understanding, superconductor technology has eventually been put into applications. Since the critical temperature of the material obtained is moving toward a higher temperature, the cooling process has evolved from the expensive liquid helium to liquid hydrogen. Superconducting magnets are some of the most powerful magnets known today. It has been widely used in laboratories and hospitals all over the industrialized world. Some of the well known laboratories machines that adopt the application of superconductors are the, mass spectrometers and the beam-steering magnets in the particle accelerator. Magnetic Resonance Imaging, (MRI) is one of the most well known machines used in hospitals to make a thorough scanning of human bodies by using magnetic resonance. The powerful magnetic fields in these applications are generated by superconductors. Modern electronics is all about thin film technology

The discovery of high-temperature superconductors with transition temperature closer to the room temperature gives a new face lift to the superconductor technology. Upon approaching the room temperature, cooling system is becoming less important in order to maintain the superconducting state. When this is eliminated, future machines and more applications can be produced with much lower cost with higher efficiency. However, much more theoretical and experimental work has to be done to achieve the cost-effective room temperature superconductor.

2.2 First Principle Method - DFT

First principles method called Density Functional Theory (DFT) was introduced by Walter Kohn around 1965. For inventing this powerful technique he was awarded the Nobel prize in Chemistry in 1998. DFT is a commonly used method in condensed-matter physics, computational Physics, material science and quantum chemistry to describe properties of condensed matter systems. DFT is a useful method to understand and predict the properties of many materials. This method allows to study materials even with minimum input parameter like the atomic type and lattice parameters, and that is why it is also called first principle method.

A rapid success has been achieved in electronic structural calculation after DFT was introduced in 1960s. Here we give a short introduction. In DFT, the assumption reduced the problem of studying a system of N electrons interacting with each other to the case of a system of N non-interacting electrons in an external potential. This was done by introducing the electronic density n(r) as the main variable instead of the full electronic wave function. The developent of DFT is based on the two theorems of Hohenberg and Kohn.

2.2.1 The Hohenberg-Kohn Theorems

First Hohenberg-Kohn theorem: The ground state density n(r) of a many-body quantum system in some external potential v(r) uniquely determine the potential.

Hence according to DFT, all properties of a many-body system can be determined by the ground state charge density:

$$\psi\{r_i, ...r_n\} \longrightarrow n(r) = \sum_i |\varphi_i(r)|^2 \tag{2.6}$$

Second Hohenberg-Kohn theorem: The ground state energy E is also uniquely determined by the ground-state charge density: the density that minimizes the

total energy is the exact ground state density.

$$E[n(r)] =< \psi|T+U+V|\psi >=< \psi|T+U|\psi >< \psi|V|\psi >= F|n(r)|+\int n(r)v(r)dr \quad (2.7)$$

Where H = T + U + V , is the many-electron Hamiltonian, ψ is ground state wave function, T is the kinetic energy, U is the electron- electron interaction, V is the external potential, and n(r) is the charge density. The universal functional F of the density is$F[n(r)] =< \psi|T + U|\psi >$. The Functional includes the kinetic energy of the electrons T_s [n], Hartree classical Coulomb repulsion energy E_H [n], and the exchange and correlation energies E_{xc} [n].

$$F[n(r)] = T_s[n] + E_H[n] + E_{xc}[n] \quad (2.8)$$

2.2.2 Kohn-Sham equation

In 1965, Kohn and Sham showed that it is possible to reduce the many-body quantum mechanical problem to an exactly equivalent set of one-electron equations, solved self-consistently. This is a reformulation of the following idea. The system of interacting electrons is mapped on to an auxiliary system of non-interacting electrons having the same ground state charge density n(r). In Kohn-Sham equation the Schrodingers equation for the system takes the following form:

$$[-\frac{\hbar^2}{2m}\nabla^2 + V(r)_{ion} + V(r)_H + V_{xc}[n(r)]]\varphi_i(r) = \epsilon_i\varphi_i(r) \quad (2.9)$$

The first term is the energy of non-interacting electrons. The second term V $(r)_ion$ is the ionic potential describing the attractive interaction between electrons and nuclei. The third term (called the Hartree potential) contains the electrostatic interactions between clouds of charge.

$$V(r)_H = \int \frac{e^2 n(r')}{|r - r'|} d^3r' \quad (2.10)$$

The fourth term is called the exchange and correlation potential.

$$V_{xc}[n(r)] = \frac{\delta E_{xc}}{\delta n(r)} \quad (2.11)$$

The nature of this external potential defines the physical properties of the system and thus is extremely important. Ground state electronic energies ϵ_i and wave functions $\varphi - i = |i, k >$ can be obtained as the result of the DFT calculation.

In many cases very good agreement with experiment is achieved when the exchange and correlation potential is treated using the rather simple local density approximation (LDA)[56,57]. A large variety of important scientific results have been and are still being obtained using LDA and the generalized gradient approximations (GGA).

2.2.3 Local Density Approximation(LDA)

Local Density Approximation is the simplest class of approximation in exchange-correlation functional. It is derived from homogeneous electron gas model. Generally, for a spin-unpolarized system, the local-density approximation for the xc energy is expressed as:

$$E_{xc}^{LDA}[n] = \varepsilon_{xc}^{hom}(n(r))n(r)dr \tag{2.12}$$

The exact exchange-correlation energy for the homogeneous electron gas was computed by Cperley and Alder using the Quantum Monte Carlo method, which was then parameterized in a functional form by Perdew and Zunger. The Local Density approximation can further be extended to an other approximation called Local Spin Density Approximation (LDA) for the treatments of magnetic materials. In this case the spin-dependence of the correlation energy density is computed by introducing the relative spin-polarization. LDA is powerful in describing many properties of systems. But it has also a limitation based on the assumption that the electron density around an atom to be homogeneous.

2.2.4 plane wave basis set and Pseudopotentials

A plane wave basis set is defined as:

$$< r|K+G| >= \frac{1}{\sqrt{V}} e^{i(K+G).r} \tag{2.13}$$

$$\frac{\hbar^2}{2m}|K+G|^2 < E_{cut} \tag{2.14}$$

where G is the reciprocal vector, V is the crystal volume, E_{cut} is a cutoff on the kinetic energy of PW's. PWs are simple to use and the basis is fixed by the crystal structure and by the cutoff. It allows to check the convergence by changing the cutoff.

The concept of Pseudopotentials have been widely applied in condensed matter Physics. The pseudopotential method is based on the fact that the valence electrons are responsible for most chemical and physical properties of molecules and solids. There are different Pseudopotentials, including norm conserving and ultrasoft.

2.2.5 Self-consistent algorithm

Fig. 2.11 schematically illustrates the major steps of a density-functional self-consistent loop. It is known that Density Functional Theory is a self-consistent field (SCF) method. This means that the calculation runs in cycles, and convergence is achieved when the results given by solving the SCF equations are consistent with the assumptions made at the beginning of the cycle. In DFT the main quantity that is calculated and checked for self-consistency, is the electronic density.

2.2.6 Brillouin zone

The Brillouin zone is important in plane-wave DFT calculations. The Brillouin zone plays an important role in electronic structure calculations. Several points in the Brillouin zone of band structures are given separate names. The

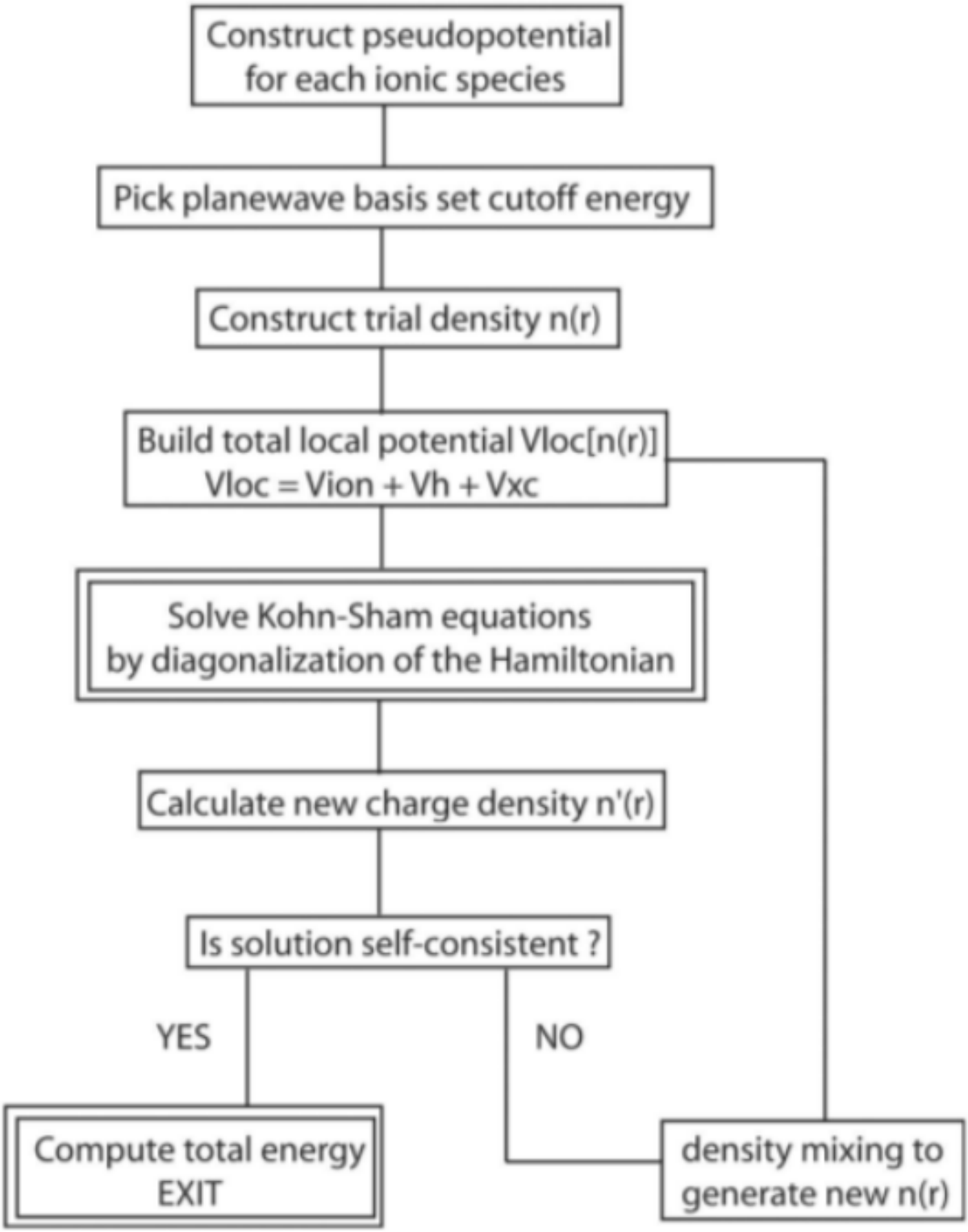

Figure 2.11: *Schematic representation of the self-consistent algorithm for a density-functional based calculation*

most important of these is where k = 0; this location in k space is called the Γ point. The volume of the primitive cell in real space defined by the WignerSeitz construction.

$$V_{BZ} = \frac{(2\pi)^3}{V_{cell}} \tag{2.15}$$

2.3 Quantum ESPRESSO

quantum ESPRESSO stands for Quantum opEn-Source Package for Research in Electronic Structure, Simulation, and Optimization[58]. Quantum ESPRESSO is an integrated suite of software for atomistic calculations based on electronic structure, using density-functional theory, a plane-wave basis set, PWscf (Plane-Wave Self-Consistent Field), pseudopotentials. Freely available under the terms of the GNU General Public License

The main goals of quantum ESPRESSO are

- innovation in methods and algorithms
- efficiency on modern computer architectures A great effort is also devoted to user friendliness and to the formation of a users' and developers' community

What can quantum ESPRESSO do ?

- Structural modeling (equilibrium structures of molecules, crystals, surfaces)
- Dynamical modeling (first-principles molecular dynamics) either on the electronic ground state (Born-Oppenheimer) or with fictitious electronic kinetic energy (Car-Parrinello)
- Chemical reactivity and transition-path sampling, using Nudged Elastic Band (NEB) method
- Linear response functions (vibrational and dielectric properties), plus some non-linear ones (third-order force constants and dielectric response)

Chapter 3

Computational methods

The calculations are performed in a plane-wave pseudopotential representation through the Quantum-Espresso (QE) program[59]. We adopt ultrasoft pseudopotentials to model the electron-ion interactions and the local-density approximation (LDA) of the exchange-correlation potential[60]. We preferred the suitable pseudo potentials for Fe, Se and Te from alternative pseudopotential library in order to obtain high quality and meaningful results on the behavior of selected correlated-electron compounds under pressure. The energy convergence is checked with respect to the cutoff energies and k-point sampling. The cutoffs for wave functions and charge density are 64Ry and 782Ry, respectively, within the framework of the density functional theory (DFT)[61] in the linear response method[45]. To obtain the structures under different pressures from 0 to 2Kbar, the initial tetragonal lattice parameters of FeSe in our calculations are based on the experimental value under ambient conditions: a = b = 3.765[a.u] , c = 5.518[a.u][1]. There are two Fe atoms and two Se atoms in the unit cell. We fully optimize the structural parameters of FeSe with increasing hydrostatic pressure by simultaneously varying the cell volume and cell parameters. It should be noted that there is no structural phase transition in the studied range of pressure. Then after, we calculate the electronic and lattice dynamical properties of FeSe based on the optimized structure and self consistent field.

The bands are plotted along the high symmetry direction in the Conventional Tetragonal-TET Brillouin zone, the lattice following the path $\Gamma - X - M - \Gamma - Z - R - A - Z$ [44] as shown in Fig 3.1. 121 k-points mesh in the Brillouin zone

was used. The DOS calculation were performed using tetrahedron method.

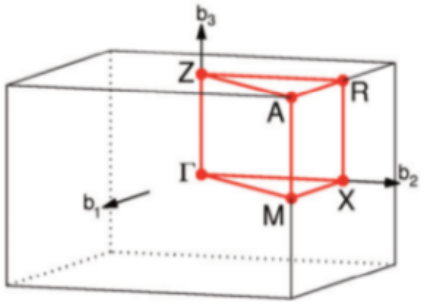

Figure 3.1: *Brillouin zone of TET with path:*$\Gamma - X - M - \Gamma - Z - R - A - Z$

In this research, we focused more on the effect of pressure to calculate transition temperature. We describe our computational methods and give structural parameters obtained by a geometry optimization under pressure for FeSe compositions in the tetragonal phase of the PbO-type (P4/nmm). The results of band structure calculations corresponding to ambient and higher pressures are presented. We used LaTeX to write the thesis, grace software to plot the band structure, DOS and different graphs of FeSe compound and XCrySDen software used for draw crystal structure of FeSe.

Chapter 4

Result and Discussion

4.1 Effects of Pressure

We observed large effects of a pressure on the superconducting transition temperature gave evidence of substantial changes in the electronic structure of FeSe under pressure. In order to clarify a nature of these changes, the geometry optimization was performed for the tetragonal P4/nmm structure of FeSe within the pseudopotential approach[61] and quantum ESPRESSO program[62]. In a such way, the pressure dependences of the crystal lattice parameters were calculated. These results are in a qualitative agreement with experimental data of Refs.[25, 53, 63, 64].

The pressure dependence of structural parameters were summarized in Figures.4.1 - 4.4. With increasing pressure, the lattice parameters a and c, the ratio of cell parameter c/a , volume of the material V and Fe-Se distance decreased monotonously. The Se-Fe-Se angle(α - angle) also decreased with increasing pressure. From this we know that the volume of the material depends on the lattice parameter, as lattices parameters are decreased the volume also decreases, while the transition temperature increased with increasing the pressure. Even if lattices parameters and volume of the material are fixed the pressure changed due to the site change of atomic position. This show that, how pressure sensitively correlated with the arrangement of crystal structure. Therefore the disorder of the site should strongly affect the superconducting properties of the Fe-based superconductor particularly FeSe.

Table 4.1: With constant atomic position of FeSe, the lattice parameters(a and c),volume, Fermi energy,total energy and pressure are calculated from self consistence fields.

a(a.u)	c(a.u)	v(Å^3)	EF(ev)	E_{total}(Ry)	P(Kbar)
3.70120055	5.51065005	75.490	9.3401	-564.18662406	0.00
3.70116655	5.51056650	75.487	9.3406	-564.18662389	0.04
3.70115500	5.51055000	75.486	9.3407	-564.18662383	0.05
3.70105000	5.51050500	75.482	9.3416	-564.18662349	0.12
3.70095700	5.50850500	75.450	9.3428	-564.18658477	0.46
3.70066440	5.50709500	75.419	9.3436	-564.18658476	0.85
3.70058000	5.50625000	75.404	9.3540	-564.18657673	1.04
3.70055000	5.50550000	75.390	9.3574	-564.18655945	1.35
3.70035000	5.50500500	75.366	9.3624	-564.18655129	1.76

Tables 4.1 and 4.2 shows the calculated value of Fermi energy, total energies

Table 4.2: With varying atomic position of FeSe, the lattice parameters(a and c),volume, Fermi energy, total energies and pressure are calculated from optimization.

a(a.u)	c(a.u)	v(Å^3)	EF(ev)	E_{total}(Ry)	P(Kbar)
3.683056993	5.7174730082	77.557	8.9860	-564.18793604	0.12
3.683033850	5.7173974160	77.555	8.9860	-564.18793604	0.17
3.683023793	5.7172302634	77.552	8.9861	-564.18793605	0.20
3.682106347	5.7157051703	77.493	8.9970	-564.18790470	0.61
3.682103727	5.7156395467	77.492	8.9975	-564.18790445	0.62
3.681566350	5.7147997000	77.458	9.0038	-564.18789490	0.96
3.676833615	5.4757803884	74.028	10.3256	-564.18236501	1.94

and volume of FeSe with varying lattice parameters a and c under pressure(P = 0 to 2Kbar). From this result, we observed the value of volume and Fermi energy increased while total energies decreased by small amount with increasing pressure.

Table 4.3: The ratio of lattice parameters (c/a) and pressure for FeSe in self consistent field .

c/a	p(Kbar)
1.488890	0.00
1.488876	0.04
1.488873	0.05
1.488400	0.46
1.488120	0.85
1.488060	1.04
1.487750	1.35
1.487700	1.76

Table 4.4: The ratio of lattice parameters (c/a) and pressure for FeSe in optimization.

c/a	p(Kbar)
1.5523715813	0.12
1.5523608115	0.17
1.5523208500	0.20
1.5522922566	0.61
1.5522755388	0.62
1.5522739934	0.96
1.4892652107	1.94

The c-axis is found to be the more compressible and the compressibility of this axis is furthermore seen to decrease at≈2Kbar. In contrast, the length of the a-axis decreases smoothly as the pressure increases. The c/a-ratio is plotted as a function of pressure. From table 4.3 and 4.4, we observed the ratio of cell parameter c/a decreased as pressure increased. This implies, lattice parameter c more decreased than lattice parameter a.

The pressure evolution of the lattice parameters a and c , the normalized ratio c/a and the volume V of the tetragonal phase, are presented in figure[4.1-4.4] in both scf and optimization. The c/a ratio decreases down to 1.4877 at 1.76Kbar meaning a larger compression of the structure along the stacking direction of the layers compared with the basal plane and it is consistent with the higher atom density in the ab plane.

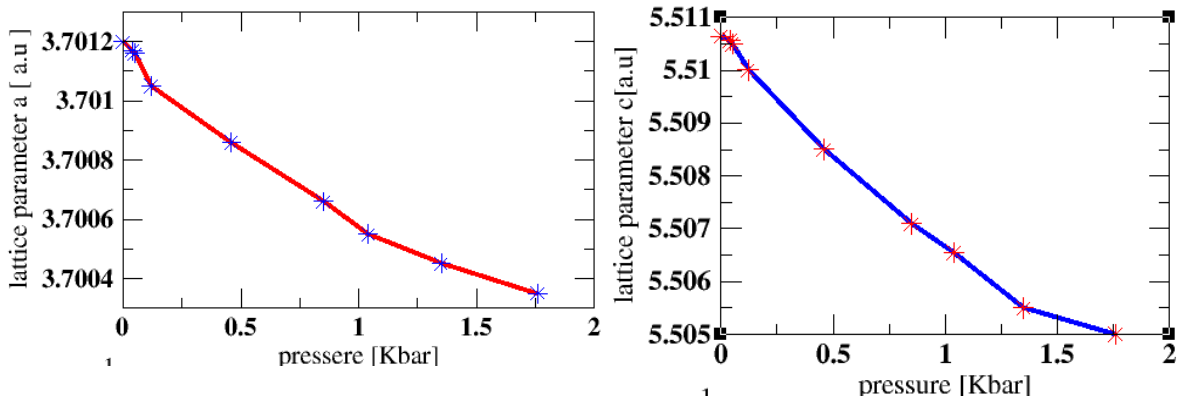

Figure 4.1: (a) The lattice parameter a[a.u] vs pressure P[Kbar] and (b) the lattice parameter c[a.u] vs pressure P[Kbar] for FeSe in scf.

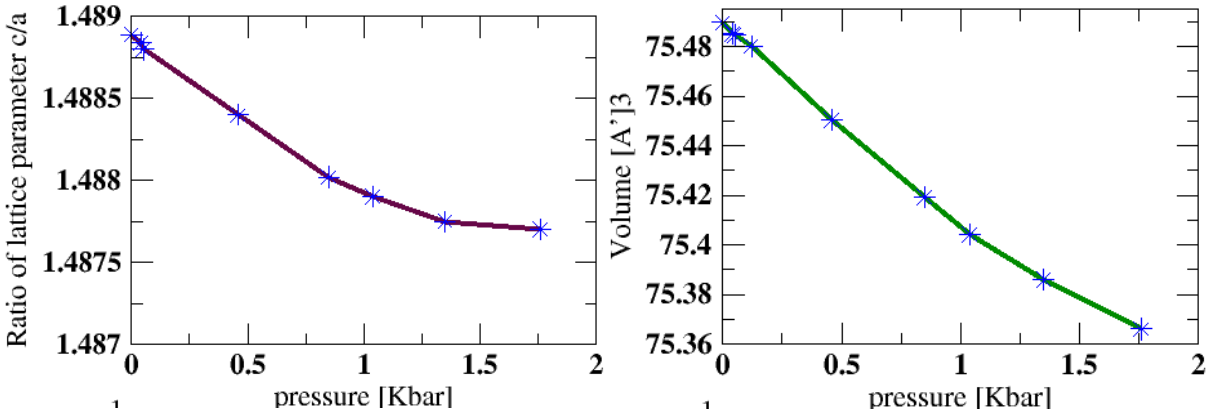

Figure 4.2: (a) The ratio of lattice parameters c/a vs pressure P[Kbar] and (b) unit cell-volume V[Å^3] vs pressure P[Kbar] for FeSe in scf.

Fig. 4.3(b) and 4.4(b) shows the unit-cell volume of FeSe plotted as function of pressure. We fitted our data with the third order Birch-Murnaghan equation of state[67]

$$P(V) = \frac{3}{2}B_0[(\frac{V_0}{V})^{\frac{7}{3}} - (\frac{V_0}{V})^{\frac{5}{3}}][1 - \frac{3}{4}(4 - B_0')[(\frac{V_0}{V})^{\frac{2}{3}} - 1]] \quad (4.1)$$

.

where V and V_0 is the volume at pressure P and zero pressure, respectively, was used for the determination of the zero pressure bulk modulus and its pressure derivative B'$_0$[66]. The obtained B_0 parameters are in good agreement with the previous experimental data[25,67,68](table 4.5). $B_o$suggest that the fitting should be done in different pressure regions. At pressure range $0 \leq$ P$<$ 2Kbar yielded B_o = 34.36GPa in optimization and 29.33GPa in case of self

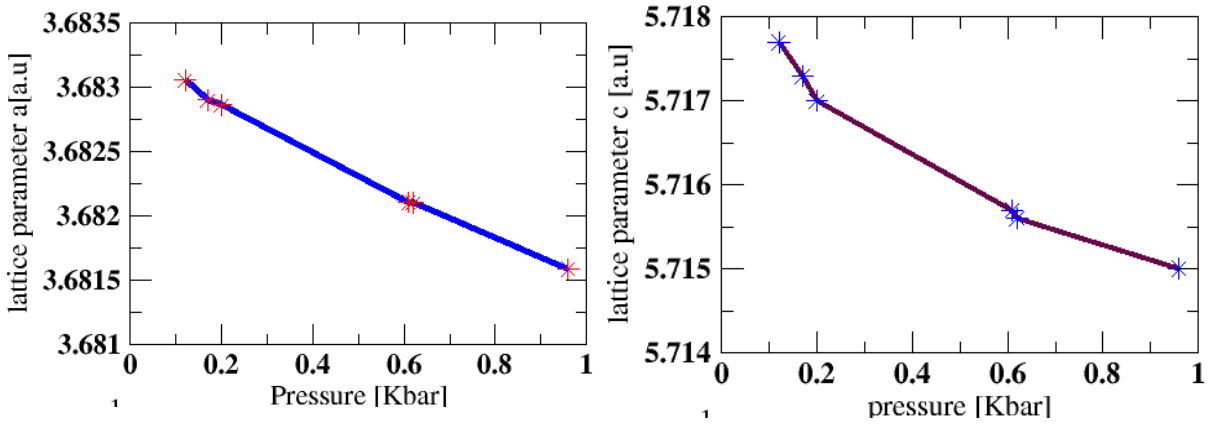

Figure 4.3: (a) The lattice parameter a[a.u] vs pressure P[Kbar] and (b) the lattice parameter c[a.u] vs pressure P[Kbar] for FeSe in VC-relax.

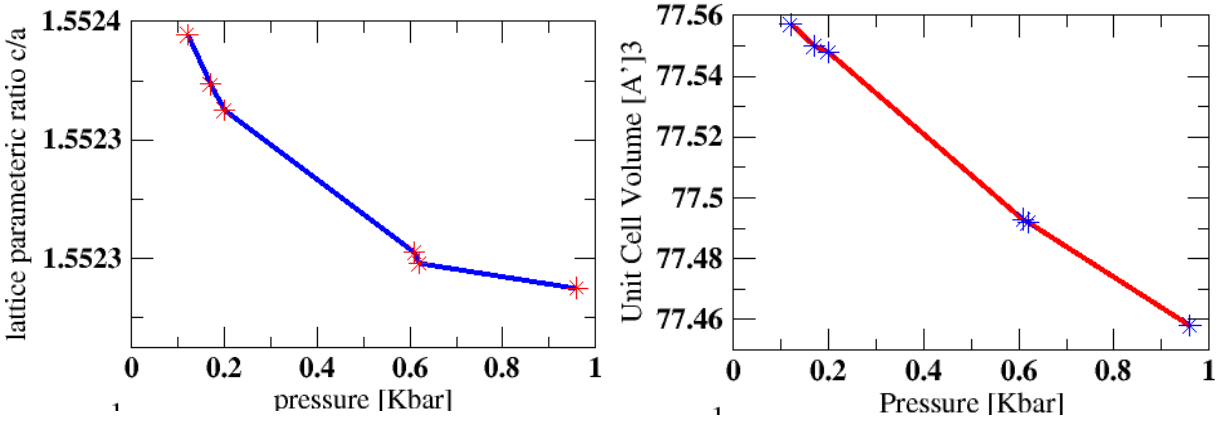

Figure 4.4: (a) The ratio of lattice parameters c/a vs pressure P[Kbar] and (b) unit cell-volume V[Å^3] vs pressure P[Kbar] for FeSe in VC-relax.

consistence field and V_0 was treated as a refinable parameter and the fit yielding V_0 = 75.49[Å^3] for scf but for vc-relax 77.56[Å^3]. This study showed the existence of a tetragonal phase with B_o = 31GPa at P = 2Kbar.

The Fermi energy has been calculated for FeSe. The Fermi energy increased with decrease the lattice parameters the [tables 4.1 and 4.2] show the correlation between Fermi energy,lattice parameter total energies and volume with pressure.

Table 4.5: The lattice parameters(a, c) ,the ratio of c/a and volume are from experimental and calculated data . The bulk moduls B_O obtained from the third-order Birch-Murnaghan equation of state(4.1)(Ref.in.65).

	a(a.u)	c(a.u)	c/a	v(Å^3)	B_0(GPa)
FeSe(exp)	3.7650	5.5180	1.4656	78.219	31
FeSe(scf)	3.7012	5.5106	1.4889	75.490	29.33
FeSe(opt)	3.683	5.7174	1.5523	77.557	34.36

4.2 DFT Computation of the Electronic Band Structure of FeSe

4.2.1 Band Structure of FeSe

The band structure of FeSe is calculated in the space group P4/nmm with non-spin polarized orbitals, in both self consistent field and optimization. The unit cell of FeSe in the space group P4/nmm consists of 2 atoms of Fe and 2 atoms of Se. The 8 Fe atoms are on the eight corners and 2 Fe atoms are on the top and bottom face centered positions as shown in Fig 3.1. The 4 Se atoms form a tetrahedron with atoms on the faces so that there are only 2 Se atoms per unit cell. The band structure for the self consistence field non-spin-polarized orbitals is given in Fig.4.5. and that for the optimization is given in Fig.4.6.

Most of the features the band structure are similar in both self consistent field and optimization structure. The Fermi energy is 9.340eV in self consistent field that would be compared with 8.986eV for the optimization one at minimum pressure. However, at high pressure p $\simeq$ 2Kbar E_F become 9.37eV and 10.32ev respectively. The band gap at various k-points is given in Table 4.6. In optimization gap varies from 0.62eV at Z point to 1.60eV at R point.

Our main results for the new electronic structure and DOS are obtained by optimizing as shown in Figure 4.6 and 4.7 respectively these are the related result with experimental value, that worked under pressure[53].
The electronic structure of FeSe near the Fermi energy contains mainly the

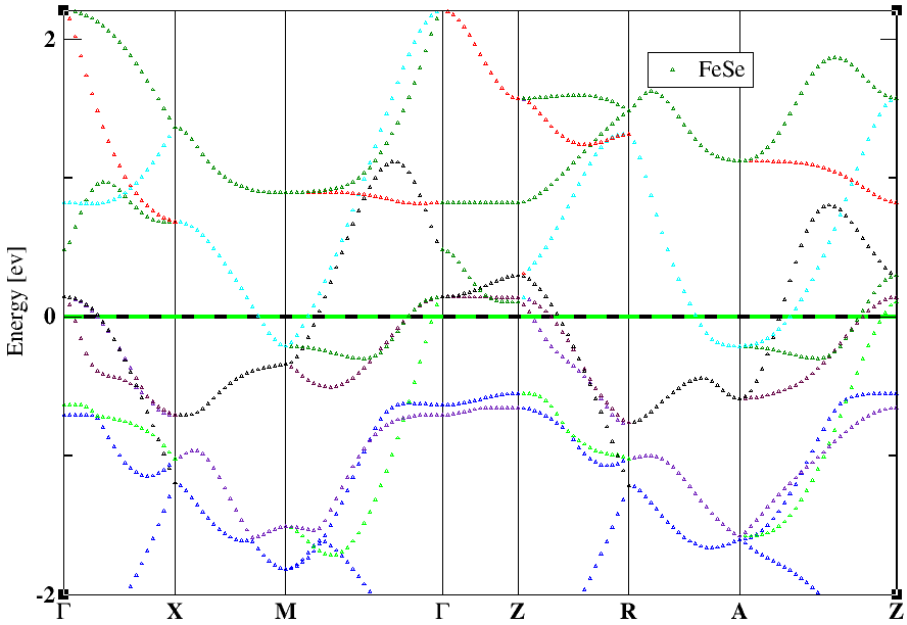

Figure 4.5: *The electronic band structures of FeSe along high- symmetry lines at p = 1.76Kbar for scf.*

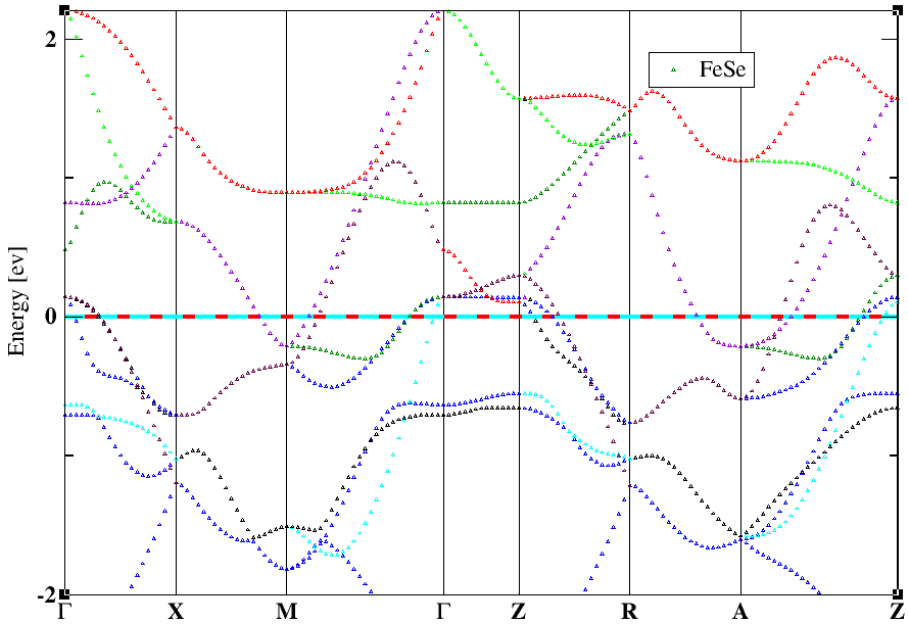

Figure 4.6: *The electronic band structures of FeSe along high- symmetry lines at p = 1.94Kbar for optimization.*

Table 4.6: The band gaps in FeSe in units of eV

	Band Gap in FeSe (eV)	
K-point	**vc-relax**	**scf**
Γ	0.71	0.72
X	0.89	0.88
M	0.67	0.72
Γ	0.71	0.72
Z	0.62	0.64
R	1.60	0.63
A	1.23	1.21
Z	0.59	0.61

Fe-3d states as can be seen from the distinct orbital character of bands as well as orbital-projected densities (FeSe at p $\cong$ 2Kbar) of states (DOS). However, the bands at the Fermi level (E_F) have also contributions from the p z orbitals, which indicates that Se-p orbitals may play a substantial role in superconductivity. This suggest the increase of electronic density. The density's at the Fermi energy are slightly enhanced under pressure. Zero pressure values of DOS at E_F are 2.69(state/cell)eV^{-1} while at pressures corresponding to the maximum critical temperature, the density's equal to 3.54(state/cell/ev) (p$\cong$ 2Kbar).

FeSe shows the most dramatic pressure dependence of T_c among the Fe based compounds. The T_c of FeSe at ambient pressure is 8K[53]. The pressure dependence of T_c had an anomaly at 1-2Kbar and the T_c increases. We calculated T_c based on McMillan equation(eqn.2.4)[32] for the superconducting transition in FeSe at 8K and using the experimental value of Debye temperature (Θ_D = 210K) which suggested in ref.[34]. According to the results of calculations of the electronic structure and the magnetic susceptibility in the normal state in an external magnetic field, FeSe compound is very close to a magnetic instability with the dominating exchange-enhanced spin paramagnetism χ_{spin} . Within the Stoner model, the exchange-enhanced Pauli spin contribution to the magnetic susceptibility can be presented as χ_{ston} = Sμ_B^2N(E_F), where S - the Stoner factor, N(E_F) - the density of states at the Fermi level, μ_B - the Bohr

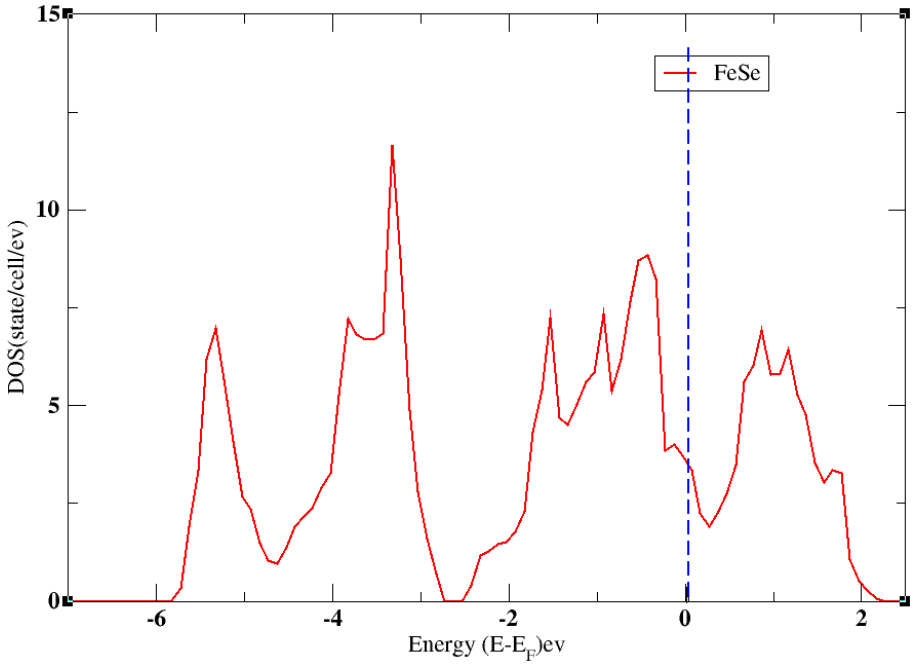

Figure 4.7: *Density of electronic states N (E) of FeSe at P = 1.94Kbar. The Fermi level (E = 0) is marked by the vertical broken line.*

magneton. The calculated value of DOS at the Fermi level for FeSe amounts to N(E_F)$\simeq$ 3.54 states/(eV.cell), allowing a small uncertainty in the determination of lattice parameters. Using the experimental value of susceptibility of FeSe at low temperatures, $\chi \simeq 1.6 \times 10^{-4}$ emu/mol [53], we obtained the Stoner factor S $\simeq$ 1.4. the corresponding parameter of renormalization of the effective masses amounts to $\lambda \simeq$ 1.4, it is possible to estimate the corresponding electron-phonon interaction parameter, $\lambda_{el-ph} \simeq$ 0.9. However, it is necessary to consider also the spin-fluctuation term, according to $\lambda = \lambda_{el-ph} + \lambda_{sf}$, which gives $\lambda_{sf} \simeq$ 0.5. and we incorporate the density of state to calculate μ^* - Coulomb's pseudopotential, in the equation (2.5),[ref. in[34]. The calculated value of critical temperature, T_c = 16.75K at pressure P$\simeq$2Kbar. The calculated result is in good agreement with both theoretical and experimental studies under pressure as shown in table 2.1[43].

Chapter 5

Conclusions

We make a calculation and simulations to obtain a band structure and DOS with QE code. We have studied the effect of external pressure on both crystal and electronic structures of FeSe superconductors. The pressure dependence of the lattice parameters a and c are shown in Figures.4.1-4.4. The c-axis is found to be the more shortened and the shortness of this axis is furthermore seen to decrease at≈2Kbar. In contrast, the length of the a-axis decreases smoothly as the pressure increases. The c/a-ratio is plotted as a function of pressure. The Correlations between pressure and lattice parameters is vary sensitive to the causes of change in volume and Fermi energy were observed. So, as pressure increase volume would be decreased while the value of T_C raised. From our calculation, we seen that a higher DOS at the Fermi level is observed under pressure. The density of state at the Fermi energy are slightly enhanced under pressure. Zero pressure values of DOS at E_F is 2.69(state/cell/ev) while at pressures corresponding to the maximum critical temperature, the density's equal to 3.54(state/cell/eV) (p≅2Kbar), which usually improves superconducting properties.

In general, we confirm the strong increase in T_C for FeSe, with an optimum value of about 16.75K and extensive calculation of the band gap in Fe_2Se_2, indicates that the transition temperature of the superconductor increases with reduced normal state gap. The Calculated T_C result shows superconductivity can be achieved only for a strong paring potential, which can not be explained by BCS type pairing.

Bibliography

[1] Tinkham M.(1996) Introduction to Superconductivity. 2nd edition, Mc Graw Hill, Inc. United States of America.

[2] F.C. Hsu et al., Proc. Natl. Acad. Sci. **105**, 14262 (2008)

[3] Nagao H et al., Int. J. Mod. Phys.**B16**,3419(2002)

[4] T. Kondo et al., Phys. Rev. Lett. **101**, 147003 (2008).

[5] W. Meissner et al., Naturwiss. **21**, 1787 (1933)

[6] T. Imai et al., Phys Rev Lett. **102** (2009).

[7] A. Subedi et al., Phys. Rev. **B 78**, 134514 (2008).

[8] B. T. Matthias, Phys. Rev. **B 92**, 874 (1953).

[9] B. T. Matthias, Phys. Rev. **B 97**, 74 (1955).

[10] L. D. Jennings and C. A. Swenson, Phys. Rev. **112**, 31 (1958).

[11] J. Hatton, Phys. Rev. **103**, 1167 (1956).

[12] C. W. Chu et al., Phys. Rev. Letters **20**, 198 (1968).

[13] P. B. Allen and M. L. Cohen, Phys. Rev. **187**, 525 (1969).

[14] K. M. Lang et al., J. Low Temp. Phys. **114**, 445 (1999).

[15] N. E. Christensen and D. L.Novikov, Phys. Rev.Letters. **86**,1861(2001).

[16] T. H. Lin and K. J. Dunn, Phys. Rev. **B 33**, 807 (1986).

[17] K. Shimizu et al., Nature (London) **419**, 597 (2002).

[18] V. Struzhkin et al., Science **298**, 1213 (2002).

[19] S. Deemyad and J.S.Schilling, Phys.Rev. Letters **91**, 167001 (2003).

[20] N. W. Ashcroft, Phys. Rev. Letters **26**, 1748 (1968).

[21] V.L.Ginzburg and L.D.Landau, Zh.Eksp.Teor. Fiz. **20**,1064(1950).

[22] J.G. Bednorz and K.A. Mueller, Z. Phys. **B64** (2), 189-193 (1986)

[23] M.A.Afrassa et al.,Physical Review **B 94**,054508(2016)

[24] M. A. Afrassa et al., Physical Review **B 92**,020505(R)(2015)

[25] J. N. Millican et al., Solid State Commun. **149**, 707 (2009).

[26] Kawashima Y. AIP Advanced, **3** (5), P. 052132(2013)

[27] A.D.Beath and D.H.Ryan phy.Review **B.76**, 064410(2007).

[28] J. Bardeen, L.N.Cooper, and J.R.Schrieffer, Phys.Rev.**108**,1175(1957)

[29] G. M. Eliashberg, Soviet Phys.-JEPT **11**, 696 (1960); **12**, 1000 (1961).

[30] J. P. Carbotte, Rev. Mod. Phys. **62**, 1027 (1990).

[31] P. Morel and P. W. Anderson, Phys. Rev. **125**, 1263 (1962).

[32] W. L. McMillan, Phys. Rev. **167**, 331 (1967).

[33] S. Medvedev et al., Nat. Mater.**8**, 630 (2009).

[34] Alexander P.Koufos et al., Phys. Rev**B 89**, 035150 (2014).

[35] S. Masaki et al., J. Phys. Soc. Jpn.**78**, 063704 (2009). Copyright 2009.

[36] Kamihara et al.,Journal of the American Chemical Society **130**, 3296 - 3297(2008)

[37] Cao Wang et al.,EPL **83**, 67006 (2008).

[38] Hiraku Ogino set al.,Supercond. Sci.Technol.**22**, 075008 (2009).

[39] Shinya Sato Supercond. Sci. Technol **23**, 045001 (2010).

[40] Jiangang Guoet al., Phys. Rev.**B 82**, 180520(R)(2010).

[41] A. Wang Phys. Rev. **B 83**, 060512(R)(2011).

[42] Johnpierre Paglione Nat Phys,advance on-line publication A.A.Kordyuk, Low teemperature physics **38** (9),(2012).

[43] M.D. Lumsden et al., arXiv:1004.1969 [cond-mat.supr-con], April 2010.

[44] Hiroki Takahashi et al., Nature 453, 376-378 (2008).

[45] Hong-Yan Ln et al.,J Low Temp Phys **178**,355 - 366 (2015)

[46] Roslova M.V.,Lebedev O.I., et al.Inorg. Chem.**52**,P.14419-14427 (2013).

[47] Grinenko V.V., Efremov D.V., et al. Physical Review **B 89**,P. 060504(R)(2014).

[48] Wurmeh S.,Lebedev O.,et al.Journal RFBR, **81**(1),P.64-76(in Russian)(2014).

[49] X. C. Wang et al., Solid State Commun. **148**, 538 (2008).

[50] H. Ogino et al., Supercond. Sci. Technol. **22**, 075008 (2009).

[51] X. Zhu et al., Phys. Rev. **B 79**, 220512 (2009).

[52] A. Subedi et al., Phys. Rev. **B 78**, 134514 (2008).

[53] G.E.Grechnev et al.,SSN 2071-0186. Ukr. J. Phys. Vol.**59**, No.3 (2014).

[54] A. N. Yaresko et al., Phys. Rev. **79**, 144421 (2009).

[55] Michael J Mehl, conduced matter superconductor. Vol.2, 1311-5914 (2014)

[56] L. Boeri, O. V. Dolgov,et al., Phys.Rev. Lett. **101**, (2), 02643 (2008).

[57] A.D. Christianson, et al., Phys. Reiv. Lett. **101** (15), 157004(2008).

[58] S. Mandal et al., Phys. Rev. **B 89**, 220502 (2014).

[59] P. Giannozzi et al., J. Phys. Condens. Matter **21**, 395502 (2009)

[60] L. Boeri et al.,Phys. Rev. **B 82**, 020506 (2010)

[61] S. Baroni et al., Rev. Mod. Phys. **73**, 515 (2001)

[62] J.P.Perdew, K.Burke, and M.Ernzerhof, Phys. Rev. Lett.**77**, 3865(1996).

[63] Drozdov A.P., Eremets M.I., et al. Nature, **525**, P.73-76(2015)

[64] R.S. Kumar et al., J. Phys. Chem. **B 114**, 12597 (2010).

[65] F. Birch, Phys. Rev. **71**, 809 (1947).

[66] A. Subedi et al., Phys. Rev. **B 78**, 134514 (2008).

[67] S. Margadonna et al., Phys. Rev. **B 80**, 064506 (2009).

[68] N. C. Gresty et al., J. Am. Chem. Soc. **131**, 16944 (2009).